The Comparative Effects of Schwann Cells and Wharton's Jelly Mesenchymal Stem Cells on the AIM2 Inflammasome Activity in Animal Model of Spinal Cord Injury

Ebrahim Kharazinejad
Abadan University of Medical Sciences
Gholamreza Hassanzadeh
Tehran University of Medical Sciences
Keywan Mortezaee
Kurdistan University of Medical Sciences
Behpour Yousefi
Semnan University of Medical Sciences and Health Services
Jamal Majidpoor
Gonabad University of Medical Sciences
Ehsan Golchini
Iranshahr University of Medical Sciences
Vajihe Taghdiri Nooshabad
Semnan University of Medical Sciences and Health Services
Mahboubeh Mousavi (Msmousavi85@gmail.com)
Semnan University of Medical Sciences and Health Services https://orcid.org/0000-0001-7490-2435

Research Article

Keywords: spinal cord injury (SCI), AIM2, inflammation, Schwann cells (SCs), Wharton's jelly mesenchymal stem cells (WJ-MSCs)

Posted Date: February 9th, 2022

DOI: https://doi.org/10.21203/rs.3.rs-1329997/v1

Version of Record: A version of this preprint was published at Neuroscience on December 15th, 2023. See the published version at https://doi.org/10.1016/j.neuroscience.2023.10.011.

Abstract

Inflammasome activation and the corresponding release of pro-inflammatory cytokines are responsible for sensory/motor deficits following spinal cord injury (SCI). Schwann cells (SCs) and Wharton's jelly mesenchymal stem cells (WJ-MSCs) represent immunomodulatory activities. Here, we aimed at comparing the efficacy of the two cell sources on absent in melanoma 2 (AIM2) inflammasome complex in SCI rats. Basso, Beattie, Bresnahan (BBB) test, Nissl and Luxol fast blue (LFB) staining were performed to assess locomotor function, neuronal survival and myelination, respectively. Gene and protein expressions of inflammasome components including AIM2, ASC, caspase-1, interleukin-1β (IL-1β) and IL-18 were analyzed by real-time polymerase chain reaction (RT-PCR), western blotting and enzyme-linked immunosorbent assay (ELISA). Expressions of the whole evaluated factors were declined in both gene and protein levels after SC or WJ-MSC treatment, which were more conspicuous for the SCs group ($P < 0.05$). Similarly, SCs increased the rates of neuronal survival and myelination. Furthermore, cell administration caused improvement in motor recovery in both treatment groups ($P < 0.05$). Although the outcomes were not significant, these effects were more notable in the SC-treated animals. From the findings it could be concluded that SC therapy is more efficient for targeting AIM2 inflammasome activation and related inflammatory circuit in SCI experiments than that for WJ-MSCs.

Introduction

Spinal cord injury (SCI) is a hazardous damage that occurs mostly due to traumatic accidents in countries all over the world [1, 2]. The incidence rate of SCI is raising annually with the prevalence of 20.7–83 per million in the USA and 8.0–130.6 per million in Europe [3]. Following the injury, two phases of critical events are developed, which further result in motor and neurological impairments [4, 5]. These events are categorized into primary and secondary damages [6]. Primary insult is characterized by neuronal loss in the spinal cord parenchyma due to hemorrhagic necrosis. Secondary damage also occurs in most cases. This concept was first described by Allen in 1911 [7] and ranges from vascular damages, edema, neurotransmitter reposition (excitotoxicity), free radical genesis, myelin loss and neuroinflammation to late cell death in neurons and other cells within the affected site, which spread to nearby areas over time [8–10].

Neuroinflammation plays a main role in the central nervous system (CNS) injuries [11]. After a damage to the CNS, a series of multiprotein complexes called inflammasomes are activated [1, 5, 12]. These complexes are the key players of innate immune system [13]. Each inflammasome consists of a cytosolic sensor, an adaptor (apoptosis-associated speck-like protein [ASC]), and a zymogen caspase. Pattern recognition receptors (PRRs) are the sensors that recognize pathogen-associated molecular patterns (PAMPs) or damage-associated molecular patterns (DAMPs) [14]. PRRs are divided into four sub-families: Toll-like receptors (TLRs), membrane-bound, retinoic acid–inducible gene (RIG)-I-like receptors (RLRs), C-type lectins (CTLs) and the nucleotide-binding domain leucine-rich repeats (NLRs). It has been shown that several NLRs, as well as a non-NLR PRR, named absent in melanoma 2 (AIM2) form inflammasomes [15, 16]. AIM2 is a member of the hemopoietic interferon-inducible nuclear 200 (HIN200)

family of proteins [13]. AIM2 inflammasome consists of three components: AIM2, ASC and caspase-1. After activation of AIM2 by pathogenic and host ectopic double-stranded DNA, procaspase-1 cleavage, interleukin-18 (IL-18) and interleukin-1β (IL-1β) maturation, and programmed cell death (pyroptosis) occur, which finally result in exacerbation of immune responses and the subsequent neuronal death [5, 17].

Many studies are performed so far to gain an understanding of mechanisms involved in the SCI pathogenesis, and the efficacy of various therapeutics are exploited for attenuating lesion-related issues [1, 2, 18, 19]. However, there are still shortcomings in this context. One of these treatments is the use of stem- or non-stem cells [20]. Schwann cells (SCs) are the main glial cells that produce myelin sheaths in the peripheral nervous system (PNS) [21]. Myelin producing SCs are involved in the CNS repair in a variety of ways, such as production of growth factors and extracellular matrix (ECM) molecules [22], activation of macrophages for the uptake of myelin debris [23], and inhibiting or delaying glial scar formation [24]. We currently found the immunomodulatory effects of these cells on suppression of NLRP1 and NLRP3 inflammasome complexes, promotion of axonal regeneration and improvement of motor function in SCI rats [1]. Mesenchymal stem cells (MSCs) are another cellular sources for therapy [25]. Similar to SCs, MSCs have high immunosuppressive potential in inflammatory diseases of the CNS [26–28]. MSCs regulate inflammatory events through releasing factors related to the immune modulation [29]. In another study, we attested the efficacy of intrathecal transplantation of Wharton's jelly MSCs (WJ-MSCs) for suppression of NLRP1 inflammasome in an animal model of SCI [4]. These findings demonstrate that inflammasome complexes can be targeted by cell therapy. To the best of our knowledge, there is no report on the role of SCs and WJ-MSCs in regulation of the AIM2 inflammasome complex, so we designed this study to compare the efficacy of these two types of cells in the rat model of SCI.

Materials And Methods

Animals and surgical procedure

A total of 40 male Wistar rats (weighing 250-300 g) were obtained from Pasteur Institute, Tehran, Iran. All animals were kept in a standard condition (12/12 light/dark cycle), having easy access to water and food ad libitum. Experimental procedures were approved by the Ethical Committee of Semnan University of Medical Sciences (Approval ID: IR.SEMUMS.REC.1400.253). Rats were randomly classified into four groups (n = 10 in all experimental groups): sham (laminectomy), SCI, SCI + SCs and SCI + WJ-MSCs. Removal of the T10 lamina was carried out only for sham group. Rats in the SCI + SCs and SCI + MSCs groups received SCs and WJ-MSCs, respectively. Compressive SCI model was introduced as the method of spinal contusion [30]. Briefly, rats were deeply anesthetized by intraperitoneal (IP) ketamine (80 mg/kg) and xylazine (10 mg/kg) (Sigma, MO). The surgical area was shaved, muscles were dissected, and dorsal laminectomy of the T10 vertebra was applied while maintaining the dura matter. Then, the cord was exposed, and compressed by placing a 50 g weight bar with a 2.2 × 5.0 mm (11.0 mm^2) contact area for 5 minutes. Manual emptying of the bladder (twice a day until recovery) and intramuscular administration of 6 mg/kg gentamycin (Caspiantamin, Iran) were performed to avoid urine infection post-SCI.

Isolation and culture of Schwann cells

SCs were harvested from sciatic nerves Wistar rats (2-3 day-old), as our previously published work [1]. Briefly, sciatic nerves were dissected bilaterally and 1 mm nerve pieces were provided. Then, the nerve pieces were digested in an enzymatic solution containing 0.03% collagenase-1 (Sigma, Germany) and 0.25% trypsin-EDTA (Sigma, Germany) in a cell culture incubator (37°C and 5% CO_2). After centrifuging of the samples (at 2000 rpm for 3 min), they were transferred into poly-L-lysine-coated culture flasks containing feeding medium of Dulbecco's Modified Eagle's Medium/ F12 (DMEM/F12) (Gibco, USA) supplemented with 10 mL fetal calf serum (FCS) (Gibco, USA), 100 U/ml penicillin (Gibco, USA), 100 µg/ml streptomycin (Gibco, USA), 1% (v/v) N2 supplement (Thermo Fisher Scientific, USA) and 10 ng/ml fibroblast growth factor (FGF)-2 (Sigma, Germany) and placed in an incubator. Culture flasks with cellular confluence of 80-85% were passaged. We used SCs at the third passage for flow cytometry analysis or transplantation.

Isolation and culture of Wharton's jelly mesenchymal stem cells

WJ-MSCs were isolated according to the protocol in the study by Sabbaghziarani et al [27]. WJ-MSCs were obtained from newborn Wharton's jelly of the umbilical cords (Shariati hospital, Tehran, Iran) under their parents' permission. In brief, WJ-MSCs were cultured in 25-cm^2 culture flasks containing DMEM/F12 supplemented with 10% FCS, 100 U/ml penicillin and 100 µg/ml streptomycin, and placed in an incubator (95% humidity and 5% CO2). After reaching 90% confluence, the cells were dissociated with 0.25% trypsin-EDTA and used for further experiments.

Immunocytochemistry of Schwann cells

Identification of SCs was evaluated by immunocytochemistry (ICC). First, cellular fixation in 4% paraformaldehyde (pH 7.4, 15 min) was applied. After rinsing with 0.1 M PBS, they were permeabilized by Triton X-100 (0.3%), normal goat serum (1%) and PBS (0.1 M) for 30 min. Then, SCs were overnight incubated **w**ith anti-S100 primary mouse antibody (Abcam, Germany) at 4°C. Following washing with PBS, further incubation (3 h) of the cells was done with AlexaFluor 488-conjugated secondary goat anti-mouse antibody (Abcam, Germany) at room temperature. Additionally, 10 µg/ml propidium iodide (PI, Sigma, Germany) was used to counterstain the nuclei [31, 32]. Finally, SCs were investigated under a fluorescent microscope (Olympus AX 70, Japan).

Flow cytometry analysis

Surface markers were assessed by flow cytometry for evaluation of the identity and purity of SCs and WJ-MSCs. For this purpose, SCs were exposed for 30 min (at 4°C) to 1 µl of fluorochrome-conjugated monoclonal antibodies against S100 and P75 NLGFr (positive), and CD45 and Thy-1 (negative) surface cell markers (all from Invitrogen, USA). WJ-MSCs were incubated with monoclonal antibodies containing fluorochrome-conjugated rat antibodies against CD34, CD45, CD73 and CD90 (all from Sigma, MO, USA).

CD73 and CD90 antibodies were used as positive markers for WJ-MSCs, and CD34 and CD45 antibodies were used for fibroblast depletion assay. Finally, the cells were assessed by a FACS Calibur flow cytometry (BD Biosciences, USA).

CM-DiI labeling and cell transplantation

1, 1'- dioctadecyl-3, 3, 3', 3'tetramethylindocarbocyanin perchlorate (C7000, Molecular Probes™, USA) was used as a fluorescent cell tracker to assess homing of SCs and WJ-MSCs before transplantation. After detachment by 0.25% Trypsin-EDTA, cell samples were rinsed in PBS and centrifuged (for 10 min at 1500 rpm). SCs or WJ-MSCs (10^6 cells) were exposed to CM-DiI/mL medium (4 μM). Then, the cells were placed in an incubator (5% CO_2 and 95% O_2) at 37°C for 30 min. Excess dye was removed by twice washing in PBS and further centrifugation steps [33, 34]. To ensure proper labeling of the cells before injection, they were observed under a fluorescence microscope and kept on ice.

Cell transplantation was carried on day 7 post-SCI. The detailed description of procedure is in our previously published work [1]. First, SCs and WJ-MSCs were detached by 0.25% Trypsin-EDTA and centrifuged for 6 min at 4000 rpm. Then, animals were anesthetized using ketamine/xylazine and placed on a board. The back of the rats was kept in a flexion position with hind limbs left to hang off. After skin incision over L3-L5 vertebrae, fascia and paravertebral muscles were excised and retracted. In the next step, 3×10^5 CM-DiI-labeled SCs or WJ-MSCs were injected using a 10 μL Hamilton syringe (26s G needle, Hamilton, USA). Cellular homing toward lesion area was assessed by a fluorescent microscope (Olympus, Japan) at 1 week after cell delivery. Figure 1 shows the timeline of the study procedure.

For further quantitative analysis of DiI^+ SCs or WJ-$MSCs^+$ after transplantation, ten sections for each animal were counted with 50 μm intervals. From each group, four rats were assigned. In the next step, cell nuclei were stained with the Hoechst dye and photographed to detect DiI-labeled transplanted cells. Finally, DiI^+ cells associated with Hoechst-stained nuclei were counted manually.

Behavioral test

Basso, Beattie and Bresnahan (BBB) test was applied for evaluation of the locomotor activity in hind limbs [35]. Rats were placed in an open-field area and observed by two blinded examiners for 5 min. Animals were scored from 0 (complete paralysis) to 21 (normal gait). The test was performed on days 1, 3 and 7 post-SCI then once a week until the end of the experiment (week 3).

Histological staining

Rats were anesthetized and underwent transcardial perfusion with 4% paraformaldehyde in PBS (0.1 M, pH 7.4) at day 21 post-injury. Spinal cord specimens were paraffin (Merk, Germany) embedded and serial sections of the lesion epicenter (i.e., T10) were obtained (5 μm slices with 50 μm interval). In order to assay gene and protein expressions, animals were sacrificed and 0.5 cm specimens of the injury site were snap-frozen rapidly in liquid nitrogen and stored at −80°C. Hematoxylin and eosin (H&E) staining was carried out at day three post-injury to ascertain the correct SCI model.

Nissl and Luxol Fast Blue (LFB) staining were performed at 21 d post-SCI. Nissl staining was for assessment of neuronal cell density and death. For this purpose, slices were deparaffinized, stained with cresyl violet, and photographs were obtained using a digital camera (Labomed, USA). Finally, an imaging software (Soft Imaging System, Berlin, Germany) was used for counting intact neurons in the ventral horn of spinal cord. LFB staining was performed to observe myelinated areas. After overnight incubation with LFB solution at 60 ºC, slices were rinsed in dH_2O and exposed to the carbonate lithium for 10 sec. Finally, samples were incubated in cresyl violet for 5 min and detected using a light microscope (Olympus, Tokyo, Japan). ImageJ Software (Soft Imaging System, Berlin, Germany) was used for measurement of diffusion of myelin outside of the site of injury.

Quantitative real-time polymerase chain reaction

Expressions of AIM2, ASC, active caspase-1, IL-18 and IL-1β genes were assessed by real-time polymerase chain reaction (RT-PCR) (n = 4 per group, 3-replica). Total RNA was extracted from tissue samples (10 mm long) including lesion site based on the manufacturer's protocols. Then, the purity of the extracted RNA was measured using a NanoDrop 1000 instrument (PeqLap, Germany). In the next step, complementary DNA (cDNA) was synthesized from the total RNA of each specimen (1 µg) by RevertAid First Strand cDNA Synthesis Kit (Thermo Scientific, USA). Relative quantification and normalization of values was calculated by a ΔΔCt method. Finally, gene expression rates were normalized to the rates of glyceraldehyde-3-phosphate dehydrogenase (GAPDH) as housekeeping and compared to the sham group. List of primers of RT-PCR are presented in the Table 1.

Table 1
List of primers

Primer	Sequence
AIM2	
F	GATGAGTTGGGCATGGGATGGT
R	TGCACTTAAAGGGTGGGGGTGG
ASC	
F	GGAGGGGTATGGCTTGGA
R	TGTTCTGTTCTGGCTGTGC
Casp-1	
F	CGTCTTGCCCTCATTATC
R	ATTCTTTTGTCATCTCCAG
IL-1b	
F	TCACTCATTGTGGCTGTGG
R	GGACGGGCTCTTCTTCAA
IL-18	
F	ATGTCTACCCTCTCCTGT
R	TTCCATTTTGTTGTGTCCTG
GAPDH	
F	AAGTTCAACGGCACAGTCAAGG
R	CATACTCAGCACCAGCATCACC

F, forward; R, reverse; *AIM2*, absent in melanoma 2; *ASC*, apoptosis-associated speck-like protein containing a caspase activation; *Casp-1, c*aspase-1; *TNF-α*, tumor necrosis factor; *IL-1β*, interleukin-1 beta; *IL-18*, interleukin-18; and *GAPDH*, glyceraldehyde-3-phosphate dehydrogenase.

Western blotting

Protein expressions of AIM2, ASC, active caspase-1, IL-18 and IL-1β were evaluated by western blot technique. Lysis buffer was added to the specimens in order to extract total proteins. Lysis buffer includes 1% (v/v) Nonidet P-40 (Sigma, Igepal, CA), 50 mM Tris–HCl, pH 8.0, 0.1% sodium dodecyl sulfate (SDS), protease inhibitor cocktail and sodium deoxycholate (Roche, Mannheim, Germany). Total Protein Kit, Micro (Sigma, USA) was used for assessment of the protein concentrations. These proteins were carried to the polyvinylidene difluoride (PVDF) membranes (Sigma, USA) for electrophoresis and then

incubated in a blocking buffer including 1 ml glycerol, 40 mL Tris-buffered saline (TBS) 1X, 20 µL Tween 20 (T) and 1 g skimmed milk for blocking unspecific proteins. Then, the membrane was exposed overnight to the primary antibodies at 4°C followed by 90 min exposure to the goat anti-rabbit secondary antibody conjugated with horseradish peroxidase (Abcam, Germany) at 37°C. The chemiluminescence method (Pierce Scientific, Waltham, MA, USA) was applied to detect target bands. Densitometric quantifications were carried out by ImageJ Software and normalized to the GAPDH. Table 2 shows the list of antibodies and molecular weight of proteins used in western blot.

Table 2
List of antibodies used in western blot

Antibody	Company	Cat. Number	molecular weight (kDA)
AIM2	Proteintech Group, USA	20590-1-AP	40
ASC	Proteintech Group, USA	10500-1-AP	23
active-caspase-1	Santa Cruz, USA	SC-56036	45
GAPDH	Sigma Aldrich	G8795	37
IL-1β	Proteintech Group, USA	16806-1-AP	30
IL-18	Proteintech Group, USA	10663-1-AP	22

Enzyme-linked immunosorbent assay

Serum levels of IL-18 and IL-1β cytokines were measured by enzyme-linked immunosorbent assay (ELISA). Blood samples (2 mL) were obtained and centrifuged (for 20 min at 2000 rpm at 4°C) before animal scarification. Next, the collected sera were analyzed using an ELISA kit (ZellBio, GmbH, Germany) for cytokine detection (cat. no. for IL-18, ZB-10073S-R9648; and for IL-1β, ZB-10055S-R9648).

Statistical analysis

Data were analyzed by one-way analysis of variance (ANOVA) followed by Tukey's post-hoc test using SPSS 24 Software. Data are presented as mean ± standard deviation (SD), and the significance level was considered as $P < 0.05$.

Results

Morphology and identity of Schwann cells and Wharton's jelly mesenchymal stem cells

After three weeks of isolation, cultured SCs showed a typical morphology of a bipolar or tripolar cell shape (Figure 2a). The identity of SCs was confirmed by tracing S100 via ICC staining (Figure 2b). The purity of SCs was 96% ± 0.3. Along with ICC, flow cytometry was used for cell identity. Results showed that the isolated cells were positive for S100 (95.52%) and P75 NLGFr (94.04%), but negative for CD45 (3.85%) and Thy-1 (4.06%) (both fibroblast markers) (Figure 2c). WJ-MSCs were investigated at week three after culturing, and the adherent cells exhibited fibroblast-like morphology (spindle shape) (Figure 2d). In addition, flow cytometry analysis showed high expressions of CD73 (95.70%) and CD90 (96.77%), but low expressions of CD34 (6.84%) and CD45 (5.09%), which are indicative of the MSC identity of the cells (Figure 2e).

Confirmation of spinal cord injury model and tracing the homing of transplanted cells

H&E staining was carried out at day three post-SCI to confirm the correct SCI induction. Cavity formation as cystic areas and bleeding in the lesion area were developed after SCI induction (Figure 3a). Administrated SCs and WJ-MSCs were detected as bright red cells under the fluorescent microscope, which confirmed the survival and correct homing of the cells into damaged areas. Quantification of the data showed that the number of DiI-labeled cells were more pronounced in the SCs group compared to the WJ-MSCs group, and that SCs were more attracted toward the site of injury (vs. WJ-MSCs, $P < 0.01$). This is indicative of the more homing and survival potential of SCs (Figure 3b).

Assessment of locomotor function, neuronal survival and myelination

BBB locomotion test was used for assessment of motor function and recovery. The highest BBB score (i.e., 21) was found in the sham group, while the lowest score was observed in the SCI group, which confirms the correct SCI model in animals. Cell therapy led to a significant improvement in locomotor activity for both SCs and WJ-MSCs groups with the respective mean scores of 14.91 and 13.89 at day 21, which were significant compared to that for the SCI group ($P < 0.05$). However, no significant difference was observed between SCs and WJ-MSCs groups (Figure 4a).

Cellular density within spinal cord tissue samples was investigated at day 21 post-SCI using Nissl staining. Intact neurons in the spinal ventral horn of the SCI group were observable in the lowest number (vs. animals in sham group), whereas a reversed finding was found after cell injection. Quantification of data showed that the number of Nissl-positive stained cells for SCs and WJ-MSCs groups were 31.38 ± 4.79 ($P < 0.01$) and 21.37 ± 3.16 ($P < 0.05$), respectively, which were significant compared to the number for the SCI group (11.67 ± 1.74). Among groups receiving cell therapy, the number was more pronounced for the SCs group ($P < 0.05$) (Figure 4b).

LFB staining was carried out at day 21 post-SCI for analysis of myelination. The most damage to the myelin sheath and the lowest number of cells in the vacuolized area was observed in the SCI group. Myelinated growing fibers were more noticeable in the cell-treated groups. Data quantification showed a

considerable decrease in the extent of damaged area after cell therapy with 65.85 ± 4.74% for the SCs (P < 0.01 vs. SCI group) and 55.00 ± 3.31% for the WJ-MSCs group (P < 0.05 vs. SCI group). Such alterations were more considerable for the SCs-treated group compared to the WJ-MSCs group (P < 0.05) (Figure 4c).

Effects of Schwann cells and Wharton's jelly mesenchymal stem cells on AIM2 inflammasome complex

Gene expression of inflammasome components (AIM2, ASC, and active caspase-1) was assessed by real-time PCR at day 21 post-SCI. A considerable increase in the mRNA expression for all inflammasome components was seen in the SCI group with the respective 13.42 ± 0.17 (P < 0.0001), 8.98 ± 0.003 (P < 0.001), and 11.56 ± 0.004 (P < 0.001) for the AIM2, ASC and caspase-1, as compared with the sham group. mRNA levels of the IL-1β and IL-18 were also evaluated, and there was also a significant rise in the SCI group with the respective 7.81 ± 0.08 (P < 0.001) and 5.85 ± 0.03 (P < 0. 01), as compared to the sham. Such effects were abrogated after cell therapy. The respective rates of the AIM2, ASC, caspase-1, IL-1β and IL-18 for the SCs group were 5.99 ± 0.01, 3.70 ± 0.03, 5.17 ± 0.004, 4.33 ± 0.11 and 2.99 ± 0.06, and for the WJ-MSCs group were 7.13 ± 0.11, 4.50 ± 0.03, 6.77 ± 0.001, 5.08 ± 0.02 and 4.34 ± 0.07 (for AIM2, ASC and caspase-1 P < 0.01 vs. SCI, and for IL-1β and IL-18 P < 0.05 vs. SCI). The downregulatory effects on AIM2 inflammasome complex were more significant for the SCs group compared with the WJ-MSCs group (P < 0.05) (Figure 5a).

Expressions of the AIM2 inflammasome complex and pro-inflammatory cytokines were also evaluated at protein level by western blotting. Similar to the corresponding genes, protein expressions of AIM2, ASC, caspase-1, IL-1β and IL-18 showed a rise in the SCI with the respective 2.25 ± 0.03, 2.36 ± 0.05, 2.67 ± 0.003, 1.75 ± 0.01 and 1.49 ± 0.001 (P < 0.001 vs. sham), which were counteracted after cell therapy. The respective rates for the SCs group were 1.99 ± 0.001, 1.89 ± 0.12, 2.24 ± 0.06, 1.14 ± 0.001 and 1.20 ± 0.08 (for inflammasome components P < 0.001 vs. SCI and for pro-inflammatory cytokines P < 0.01 vs. SCI), and for the WJ-MSCs group were 2.12 ± 0.04, 1.98 ± 0.06, 2.05 ± 0.16, 1.45 ± 0.07 and 1.20 ± 0.06 (for both P < 0.05 vs. SCI). Again, such alterations were more pronounced in the SCs group compared to the WJ-MSCs group (P < 0.05) (Figure 5b).

Findings of enzyme-linked immunosorbent assay

Supplementary to western blot, ELISA assay was applied for analysis of the serum levels of IL-1β and IL-18. The trend for ELISA was similar to the results from western blot in which the whole protein rates were increased in the SCI group, while the alterations were significantly abrogated after cell therapy. The rates for IL-1β and IL-18 in the SCs group were 60.107 ± 0.395 ng/ml (P < 0.05 vs. SCI) and 41.235 ± 0.591 ng/ml (P < 0.01 vs. SCI), and in the WJ-MSCs group were 70.224 ± 0.679 ng/ml and 56.775 ± 0.112 ng/ml (for both P < 0.05 vs. SCI). This rise was more noticeable in the SCs group compared to the WJ-MSCs group (for both cytokines P < 0.05) (Figure 6).

Discussion

Results of the present study showed the beneficial effects of cell therapy against the destructive changes in animal model of SCI. Here, the efficacy of SCs and WJ-MSCs on myelination, motor activity and AIM2 inflammasome complex were compared. To the best of our knowledge, this is the first study assessing and comparing the effects of SCs and WJ-MSCs on the AIM2 inflammasome complex in SCI rats. Outcomes of this study showed superior roles for SCs compared to the WJ-MSCs for promoting recovery from SCI, as discussed further. Three possible reasons for preferring SCs over MSCs in cell therapy are (a) lower survival of MSCs within lesioned areas compared to the SCs, as our data showed lower number of DiI^{+} MSCs in the site of injury, (b) MSCs are less likely to differentiate into neurons and glial cells, as reported only 2% of MSCs were differentiated into astrocytes [36], and (c) different cellular sources in which SCs are a part of PNS, so they have more in common with nervous system than that for WJ-MSCs.

BBB locomotion rating scale is extensively used for measurement of motor recovery in rodents post-SCI [1]. So, we examined locomotor function of the rat hind limbs at day 21 post-SCI, and results indicated that SCI animals experienced higher motor problems. This was ameliorated after administration of either SCs or MSCs, but no remarkable differences were observed between the two treatment groups. This outcome is inconsistent with the fact that the relation between behavioral improvement in the hind limbs and white matter retention is complicated. Instead, it is attributed to the involvement of upper and lower neuronal networks, such as segmental, intersegmental and supraspinal circuitries [37]. We also performed H&E, Nissl and LFB staining to confirm SCI model, and to detect neuronal survival and myelination, respectively. H&E staining showed fewer number of cavities filled with cell accumulations in the SCs group compared to the WJ-MSCs group, and Nissl staining displayed higher number of Nissl-positive cells in the SCs group. Moreover, LFB staining showed higher number of newly myelinated axons in the treated groups with more pronounced outcomes for the SCs. There are some reports showing that SCs have the potential to augment the number of myelinated axonal fibers, to reduce the size of cavity cavities, and to increase the extent of spinal white matter [21, 38]. These findings affirm that cell therapy is effective for counteracting mechanical changes caused by SCI in ventral motor horn of spinal cord, and that the effects were sharper after administration of SCs compared to the WJ-MSCs.

AIM2 inflammasome is contributed to a number of neurological diseases including traumatic brain injury (TBI), ischemic brain injury and especially SCI [13, 39, 40]. In the intact spinal cord, AIM2 is expressed by neurons, astrocytes, microglia and oligodendrocytes. Infiltrations of leukocytes, activated astrocytes and microglia/macrophages are responsible for increased expression of this inflammasome after SCI [19]. In the present work, we found that the expressions of AIM2 inflammasome components and downstream pro-inflammatory L-1β and IL-18 were enhanced at both mRNA and protein levels after SCI induction, which was antagonized after cell therapy with sharper decline found for SCs compared to the WJ-MSCs. SCs and MSCs show immunomodulatory effects through their ability to secrete immunosuppressive factors, to modulate immune cells and to suppress pro-inflammatory cytokines, in particular [29, 41]. MSCs are able to suppress inflammasome activation through release of anti-apoptotic factors and regulation of the mediator of oxidative stress in the injured area [42]. SC therapy causes a reparative shift in the polarity of immune cells including macrophages to repress inflammation [43]. In addition, a

positive relationship was found between SCs with regulation of cytokine expression. It was found a suppressor role of SCs on pro-inflammatory cytokines in SCI rats after co-administration with olfactory ensheathing cells, which indicates that such therapy provides a modified environment for tissue repair [44]. Taken together, it could be asserted that cell therapy with exogenous SCs or WJ-MSCs is an effective approach for recovering mechanical and chemical changes occurring within the spinal cord milieu, and the superior roles taken by SCs are indicative of more accommodation of such cells with cells of spinal cord and their higher potency for modulation of inflammasomes in favor of therapy. Our suggestion for future works is to survey the efficacy of growth factors or hormones related to expansion of the life span of exogenous cells within the site of SCI, as what reported for melatonin preconditioning (melatonin is a hormone of pineal gland that shows potent anti-oxidative activity [45]) in other diseases [46, 47].

Conclusion

From the results of this study, we conclude that administration WJ-MSCs or SCs, in particular, may have potentials for ameliorating tissue devastating effects of SCI in experimental models through suppressing the activity of inflammasome complexes including AIM2 and regulation of the release of pro-inflammatory cytokines, thereby recovering neuronal damage and motor deficit in injured animals.

Declarations

Funding and Acknowledgments

This research was funded by a grant from Semnan University of Medical Sciences and Health Services, Semnan, Iran (grant number: A-10-551-1).

Competing Interests

The authors declare no potential conflicts of interest.

Authors' contributions

All authors contributed distinctly in the presented work. Conceptualization and study designing, Mahboubeh Mousavi, Ebrahim Kharazinejad and Gholamreza Hassanzadeh; Performing Experiments and data interpretation, Vajihe Taghdiri Nooshabadi and Behpour Yousefi; writing, original draft preparation, Ebrahim Kharazinejad, Keywan Mortezaee and Mahboubeh Mousavi; review and editing, Ehsan Golchini, Keywan Mortezaee and Jamal Majidpoor. Authors have read and agreed to publish the manuscript.

Data Availability statement

All data generated or analysed during this study are included in this published article.

Ethics approval

All animal-related procedures, including anesthesia and surgery, were carried out according to the national and institutional guidelines of Semnan University of Medical Science for use and care of animals in the laboratory (Approval ID: IR.SEMUMS.REC.1400.253).

Consent for publication

The authors of the paper have been read and approve and consent the final version for publication.

Consent to participate

Not applicable.

References

1. Mousavi, M., et al., *Schwann cell transplantation exerts neuroprotective roles in rat model of spinal cord injury by combating inflammasome activation and improving motor recovery and remyelination.* Metabolic brain disease, 2019. **34**(4): p. 1117-1130.
2. Majidpoor, J., et al., *The expressions of NLRP1, NLRP3, and AIM2 inflammasome complexes in the contusive spinal cord injury rat model and their responses to hormonal therapy.* Cell and Tissue Research, 2020. **381**(3): p. 397-410.
3. Yuan, S., et al., *Epidemiological features of spinal cord injury in China: a systematic review.* Frontiers in neurology, 2018. **9**: p. 683.
4. Mohamadi, Y., et al., *Intrathecal transplantation of Wharton's jelly mesenchymal stem cells suppresses the NLRP1 inflammasome in the rat model of spinal cord injury.* Journal of chemical neuroanatomy, 2019. **97**: p. 1-8.
5. Mortezaee, K., et al., *Inflammasome: its role in traumatic brain and spinal cord injury.* Journal of cellular physiology, 2018. **233**(7): p. 5160-5169.
6. Alizadeh, A., S.M. Dyck, and S. Karimi-Abdolrezaee, *Traumatic spinal cord injury: an overview of pathophysiology, models and acute injury mechanisms.* Frontiers in neurology, 2019. **10**: p. 282.
7. Allen, A.R., *Surgery of experimental lesion of spinal cord equivalent to crush injury of fracture dislocation of spinal column: a preliminary report.* Journal of the American Medical Association, 1911. **57**(11): p. 878-880.
8. Oyinbo, C.A., *Secondary injury mechanisms in traumatic spinal cord injury: a nugget of this multiply cascade.* Acta Neurobiol Exp (Wars), 2011. **71**(2): p. 281-99.
9. Alizadeh, A., *Elucidating the role of neuregulin-1 in glial and immune response following traumatic spinal cord injury.* 2018.
10. von Leden, R., et al., *Review: CNS ijury and NADPH oxidase: oxidative stress and therapeutic targets.* J Neurotrauma, 2016. **34**: p. 755-764.
11. Slowik, A., et al., *Brain inflammasomes in stroke and depressive disorders: regulation by oestrogen.* Journal of neuroendocrinology, 2018. **30**(2): p. e12482.

12. Majidpoor, J., et al., *The effect of the "segment" of spinal cord injury on the activity of the nucleotide-binding domain-like receptor protein 3 inflammasome and response to hormonal therapy.* Cell Biochemistry and Function, 2021. **39**(2): p. 267-276.
13. Adamczak, S.E., et al., *Pyroptotic neuronal cell death mediated by the AIM2 inflammasome.* Journal of Cerebral Blood Flow & Metabolism, 2014. **34**(4): p. 621-629.
14. de Rivero Vaccari, J.P., W.D. Dietrich, and R.W. Keane, *Activation and regulation of cellular inflammasomes: gaps in our knowledge for central nervous system injury.* Journal of Cerebral Blood Flow & Metabolism, 2014. **34**(3): p. 369-375.
15. Latz, E., T.S. Xiao, and A. Stutz, *Activation and regulation of the inflammasomes.* Nature Reviews Immunology, 2013. **13**(6): p. 397-411.
16. Vladimer, G.I., et al., *Inflammasomes and host defenses against bacterial infections.* Current opinion in microbiology, 2013. **16**(1): p. 23-31.
17. Rathinam, V.A., et al., *The AIM2 inflammasome is essential for host defense against cytosolic bacteria and DNA viruses.* Nature immunology, 2010. **11**(5): p. 395-402.
18. Namjoo, Z., et al., *Combined effects of rat Schwann cells and 17β-estradiol in a spinal cord injury model.* Metabolic brain disease, 2018. **33**(4): p. 1229-1242.
19. Wang, S.-N., et al., *Expression and localization of absent in melanoma 2 in the injured spinal cord.* Neural regeneration research, 2019. **14**(3): p. 542.
20. Mortazavi, M.M., et al., *Treatment of spinal cord injury: a review of engineering using neural and mesenchymal stem cells.* Clinical anatomy, 2015. **28**(1): p. 37-44.
21. Namjoo, Z., et al., *Targeting axonal degeneration and demyelination using combination administration of 17β-estradiol and Schwann cells in the rat model of spinal cord injury.* Journal of cellular biochemistry, 2018. **119**(12): p. 10195-10203.
22. Mirsky, R., et al., *Schwann cells as regulators of nerve development.* Journal of Physiology-Paris, 2002. **96**(1-2): p. 17-24.
23. Arthur-Farraj, P.J., et al., *c-Jun reprograms Schwann cells of injured nerves to generate a repair cell essential for regeneration.* Neuron, 2012. **75**(4): p. 633-647.
24. Kuo, H.-S., et al., *Acid fibroblast growth factor and peripheral nerve grafts regulate Th2 cytokine expression, macrophage activation, polyamine synthesis, and neurotrophin expression in transected rat spinal cords.* Journal of Neuroscience, 2011. **31**(11): p. 4137-4147.
25. Ide, C., et al., *Bone marrow stromal cell transplantation for treatment of sub-acute spinal cord injury in the rat.* Brain research, 2010. **1332**: p. 32-47.
26. Urdzíková, L.M., et al., *Human mesenchymal stem cells modulate inflammatory cytokines after spinal cord injury in rat.* International journal of molecular sciences, 2014. **15**(7): p. 11275-11293.
27. Sabbaghziarani, F., et al., *Retinoic acid-pretreated Wharton's jelly mesenchymal stem cells in combination with triiodothyronine improve expression of neurotrophic factors in the subventricular zone of the rat ischemic brain injury.* Metabolic brain disease, 2017. **32**(1): p. 185-193.

28. Zhang, R., et al., *Anti-inflammatory and immunomodulatory mechanisms of mesenchymal stem cell transplantation in experimental traumatic brain injury.* Journal of neuroinflammation, 2013. **10**(1): p. 1-12.
29. English, K., *Mechanisms of mesenchymal stromal cell immunomodulation.* Immunology and cell biology, 2013. **91**(1): p. 19-26.
30. Zendedel, A., et al., *Activation and regulation of NLRP3 inflammasome by intrathecal application of SDF-1a in a spinal cord injury model.* Molecular neurobiology, 2016. **53**(5): p. 3063-3075.
31. Moradi, F., et al., *BD PuraMatrix peptide hydrogel as a culture system for human fetal Schwann cells in spinal cord regeneration.* Journal of neuroscience research, 2012. **90**(12): p. 2335-2348.
32. Shen, M., et al., *A proteome map of primary cultured rat Schwann cells.* Proteome science, 2012. **10**(1): p. 1-9.
33. Kubilus, J.K. and T.F. Linsenmayer, *Developmental corneal innervation: interactions between nerves and specialized apical corneal epithelial cells.* Investigative ophthalmology & visual science, 2010. **51**(2): p. 782-789.
34. Pourheydar, B., et al., *Co-transplantation of bone marrow stromal cells with schwann cells evokes mechanical allodynia in the contusion model of spinal cord injury in rats.* Cell Journal (yakhteh), 2012. **13**(4): p. 213.
35. Basso, D.M., M.S. Beattie, and J.C. Bresnahan, *A sensitive and reliable locomotor rating scale for open field testing in rats.* Journal of neurotrauma, 1995. **12**(1): p. 1-21.
36. Ha, Y., et al., *Transplantation of human umbilical cord blood improves neurological outcomes in the rats after traumatic spinal cord injury.* Journal of Korean Neurosurgical Society, 2004. **35**(3): p. 302-308.
37. Kachadroka, S., et al., *Effect of endogenous androgens on 17 β-estradiol-mediated protection after spinal cord injury in male rats.* Journal of neurotrauma, 2010. **27**(3): p. 611-626.
38. Myers, S.A., et al., *Does the preclinical evidence for functional remyelination following myelinating cell engraftment into the injured spinal cord support progression to clinical trials?* Experimental neurology, 2016. **283**: p. 560-572.
39. de Rivero Vaccari, J.P., et al., *Therapeutic neutralization of the NLRP1 inflammasome reduces the innate immune response and improves histopathology after traumatic brain injury.* Journal of Cerebral Blood Flow & Metabolism, 2009. **29**(7): p. 1251-1261.
40. Denes, A., et al., *AIM2 and NLRC4 inflammasomes contribute with ASC to acute brain injury independently of NLRP3.* Proceedings of the National Academy of Sciences, 2015. **112**(13): p. 4050-4055.
41. Zhang, S.H., et al., *Immunomodulation by Schwann cells in disease.* Cancer Immunology, Immunotherapy, 2020. **69**(2): p. 245-253.
42. Oh, J.Y., et al., *Mesenchymal stem/stromal cells inhibit the NLRP3 inflammasome by decreasing mitochondrial reactive oxygen species.* Stem cells, 2014. **32**(6): p. 1553-1563.

43. Pearse, D.D., et al., *Schwann cell transplantation subdues the pro-inflammatory innate immune cell response after spinal cord injury.* International journal of molecular sciences, 2018. **19**(9): p. 2550.
44. Zhang, J., et al., *The effects of co-transplantation of olfactory ensheathing cells and Schwann cells on local inflammation environment in the contused spinal cord of rats.* Molecular Neurobiology, 2017. **54**(2): p. 943-953.
45. Mortezaee, K., et al., *Post-treatment of melatonin with CCl4 better reduces fibrogenic and oxidative changes in liver than melatonin co-treatment.* Journal of cellular biochemistry, 2018. **119**(2): p. 1716-1725.
46. Mortezaee, K., et al., *Melatonin pretreatment enhances the homing of bone marrow-derived mesenchymal stem cells following transplantation in a rat model of liver fibrosis.* Iranian biomedical journal, 2016. **20**(4): p. 207.
47. Mortezaee, K., et al., *Preconditioning with melatonin improves therapeutic outcomes of bone marrow-derived mesenchymal stem cells in targeting liver fibrosis induced by CCl4.* Cell and tissue research, 2017. **369**(2): p. 303-312.

Figures

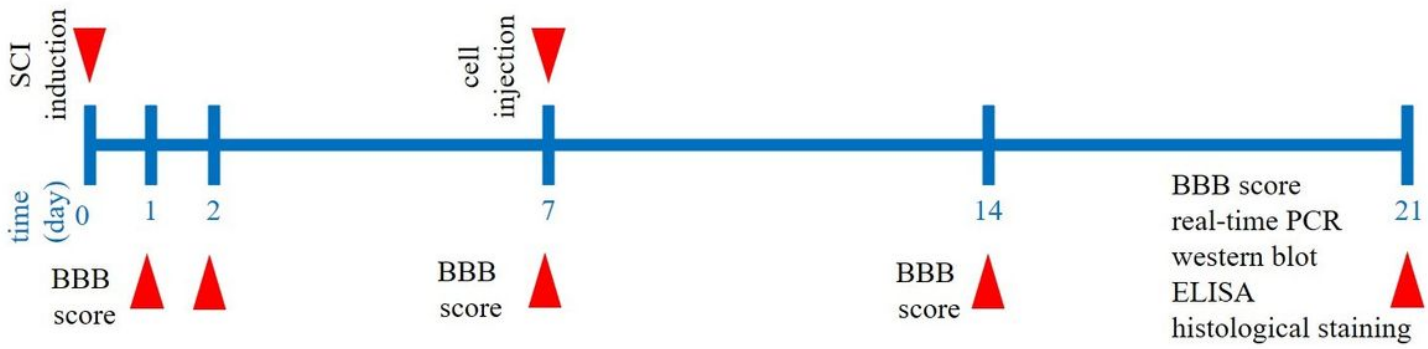

Figure 1

Timeline of experimental procedures. On day 0, spinal cord injury (SCI) was induced, and locomotor activity was assessed by Basso, Beattie and Bresnahan (BBB) test on days 1, 3, 7, 14, and 21 post-SCI. After assessment of the final BBB, animals were sacrificed. Histological staining, quantitative real-time polymerase chain reaction (PCR), western blot (WB) and enzyme-linked immunosorbent assay (ELISA) were done at this time.

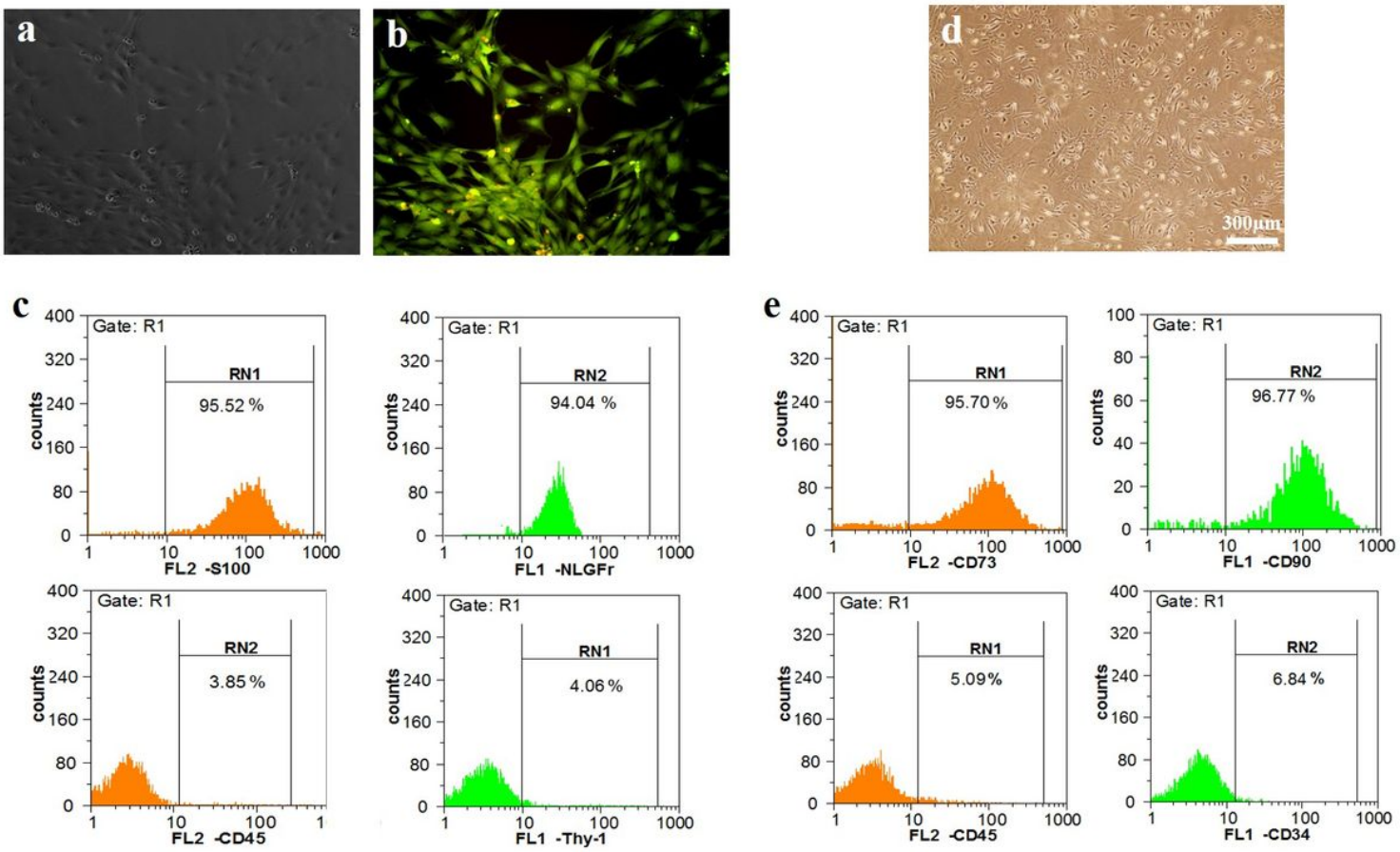

Figure 2

Morphology and identity of Schwann cells (SCs) and Wharton's jelly mesenchymal stem cells (WJ-MSCs). **(a)** Morphology of SCs. SCs showed bi- or tripolar elongated morphology. **(b)** Immunocytochemistry (ICC) of SCs. ICC was done in rat SCs by assessing anti-S100 antibody (green) and nuclei stained with propidium iodide (yellow). **(c)** Flow cytometry analysis for SC identity. SCs expressed high levels of P75 NLGFr and S100, but low levels of CD45 and CD90. **(d)** Morphology of WJ-MSCs. WJ-MSCs displayed spindle-like shape after 3 weeks of culturing. **(e)** Flow cytometry analysis for WJ-MSC identity. WJ-MSCs were positive for CD73 and CD90, but negative for CD34 and CD45.

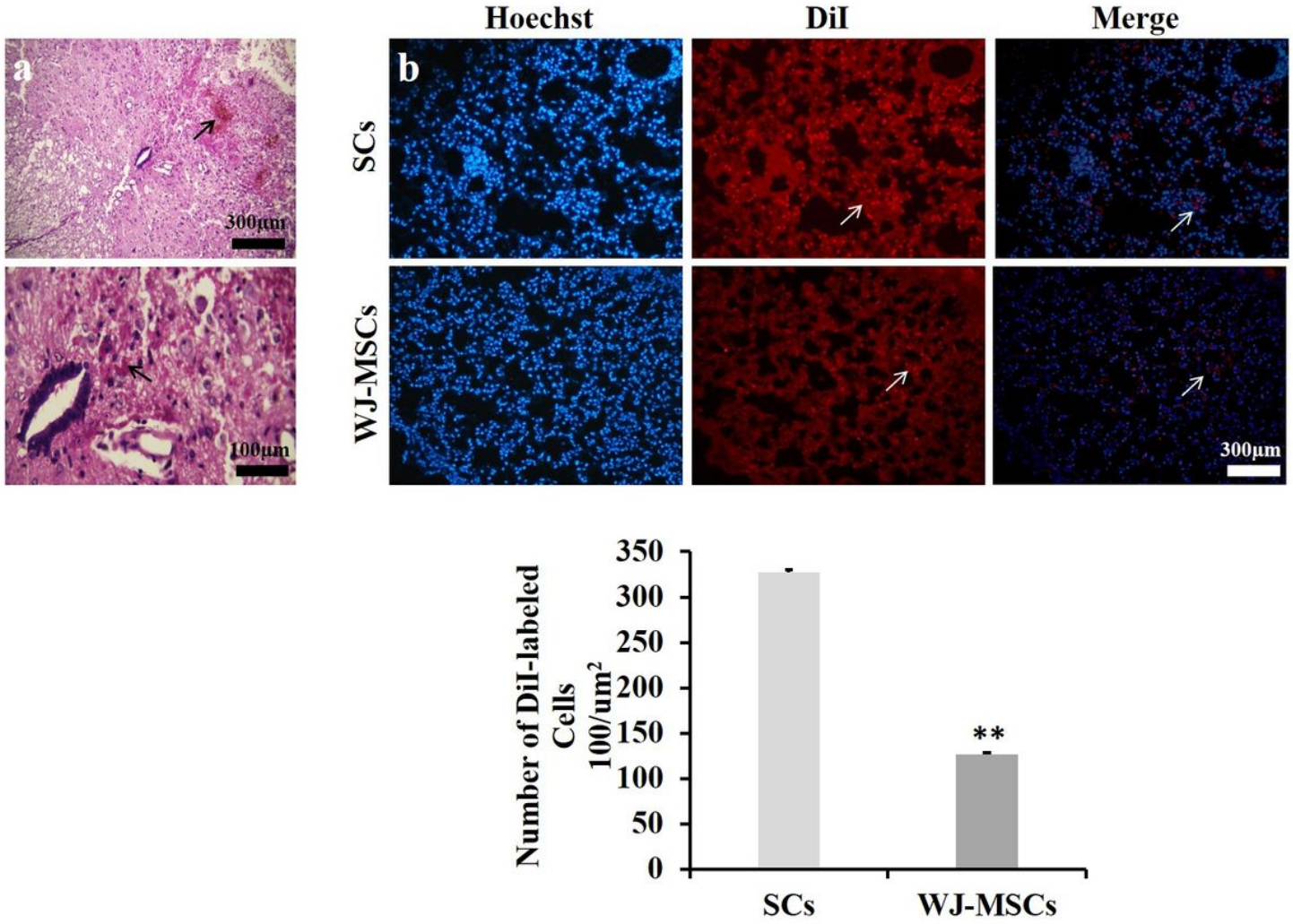

Figure 3

Confirmation of spinal cord injury model (SCI) and homing of Schwann cells (SCs) and Wharton's jelly mesenchymal stem cells (WJ-MSCs) into the injured area. **(a)** Hematoxylin and eosin (H&E). H&E showed cavities as cystic areas and bleeding in the lesion area (arrow). **(b)** Homing of grafted SCs and WJ-MSCs at one week after cell delivery. Cells were labeled with DiI and observed as bright red points in the injury site (arrows). Quantification of DiI-labeled cells showed higher number of SCs-labeled cells than WJ-MSCs-labeled cells. Data are represented as mean ± SD. $^{**}p < 0.01$ vs. SCs.

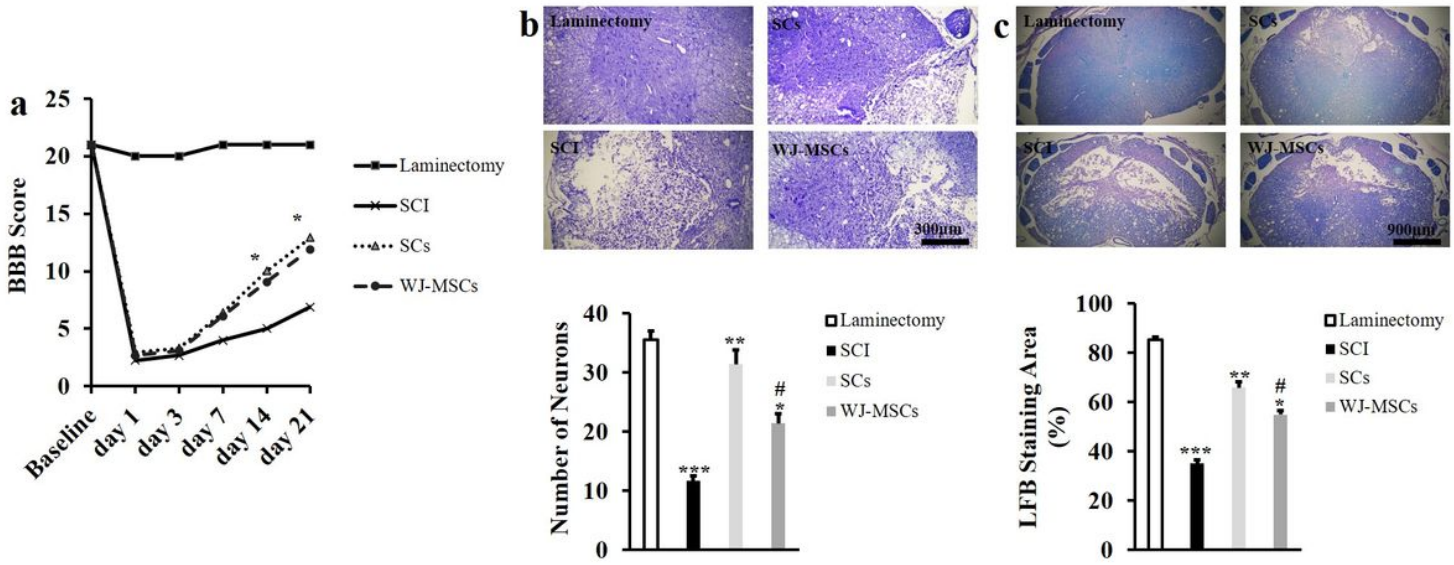

Figure 4

Evaluation of motor activity, and neuronal survival and myelination for investigating the effects of Schwann cells (SCs) and Wharton's jelly mesenchymal stem cells (WJ-MSCs) in spinal cord injury (SCI) rat model. **(a)** Basso, Beattie and Bresnahan (BBB) assessment for motor activity (n = 8 per group). No considerable difference in motor activity was found between SCs and WJ-MSCs groups. $^{*}p < 0.05$ SCs and WJ-MSCs vs. SCI. **(b)** Nissl staining for evaluation of neuronal survival (n = 5 per animal). Spinal cord ventral horn cells were evaluated for survival assay. The number of Nissl-positive stained cells was more pronounced for the SCs group, which was significant after quantification. $^{\#}p < 0.05$ vs. SCs; $^{*}p < 0.05$ vs. SCI; $^{**}p < 0.01$ vs. SCI; and $^{***}p < 0.001$ vs. laminectomy. **(c)** Luxol Fast Blue (LFB) staining for evaluation of myelination (n = 7 per group). Reduced axonal degeneration and demyelination were observed in the treatment groups. Quantification of data showed that the extent of myelinated areas was significantly higher in SCs vs. WJ-MSCs. $^{\#}p < 0.05$ vs. SCs; $^{*}p < 0.05$ vs. SCI; $^{**}p < 0.01$ vs. SCI; and $^{***}p < 0.001$ vs. laminectomy. For all tests, data are represented as mean ± SD.

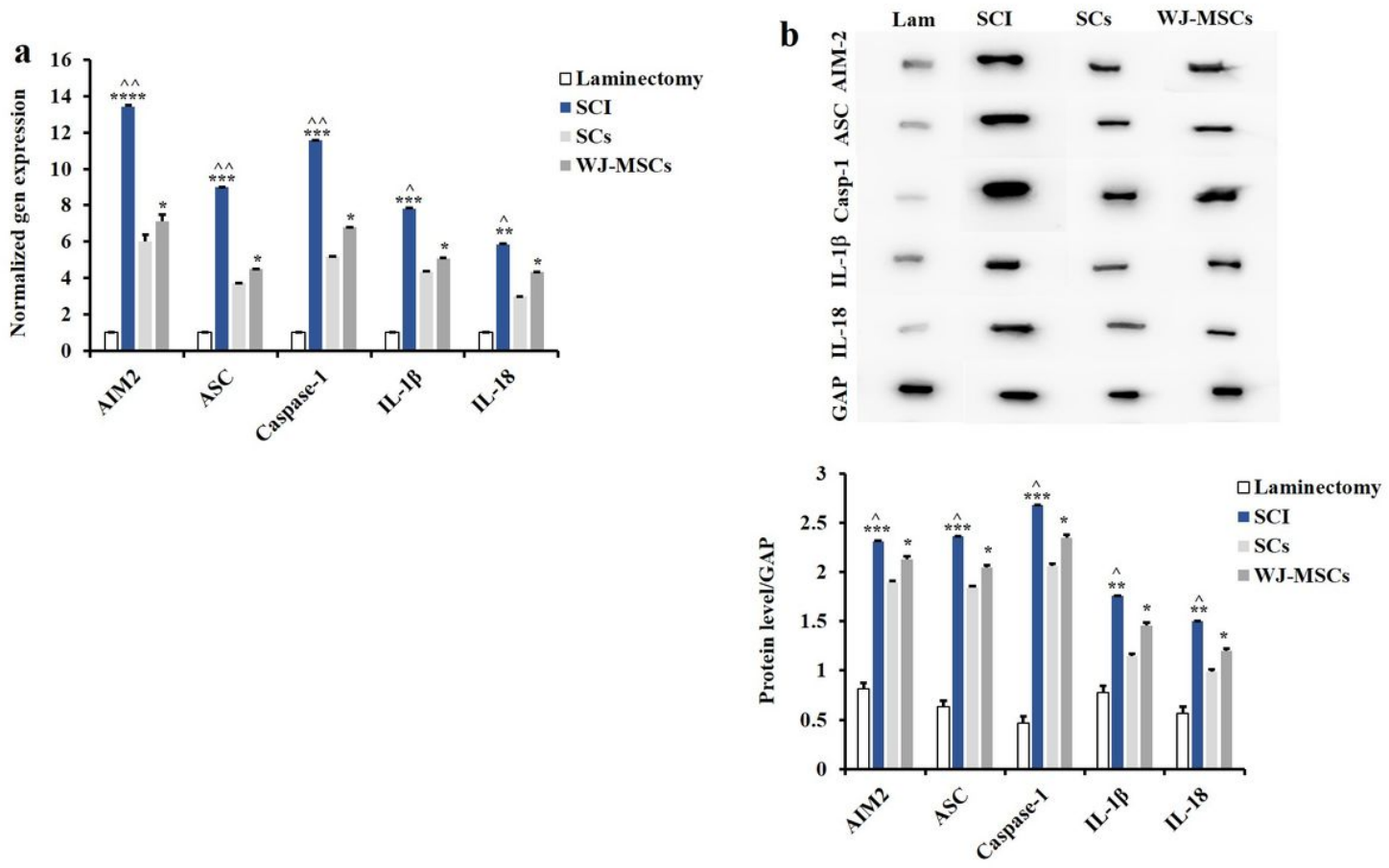

Figure 5

Evaluation of the AIM2 inflammasome complex at gene and protein levels for evaluation of the impact of Schwann cells (SCs) and Wharton's jelly mesenchymal stem cells (WJ-MSCs) in spinal cord injury (SCI) rat model. **(a)** Quantitative real-time PCR (qRT-PCR) for assessment of gene expressions related to the absent in melanoma 2 (AIM2) inflammasome complex (n = 5). GAPDH was used as a housekeeping gene. **(b)** Western blot for assessment of gene expressions related to the AIM2 inflammasome complex (n = 4). AIM2, ASC, and active caspase-1, interleukin (IL)-1β and IL-18 were highly expressed at gene and protein levels in SCI, but such expression was counteracted after cell therapy with sharper decrease was found for the SCs group. "Lam" is the abbreviation for "Laminectomy". Data are expressed as mean ± SD. $^{\wedge}p < 0.05$ vs. SCs and MSCs; $^{*}p < 0.05$ vs. SCs; $^{**}p < 0.01$ vs. laminectomy; $^{\wedge\wedge}p < 0.01$ vs. SCs and MSCs; and $^{***}p < 0.001$ vs. laminectomy; and $^{****}p < 0.0001$ vs. laminectomy

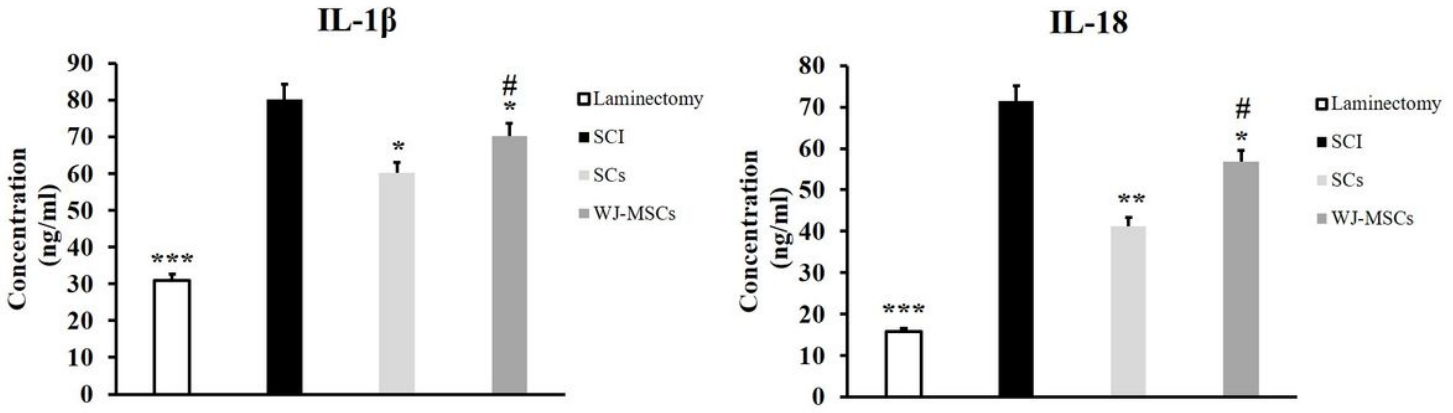

Figure 6

Enzyme-linked immunosorbent assay (ELISA) for evaluation of the protein expressions of interleukin (IL)-1β and IL-18 in the spinal cord injury (SCI) rats for investigating the impact of Schwann cells (SCs) and Wharton's jelly mesenchymal stem cells (WJ-MSCs). $^{\#}p < 0.05$ vs. SCs; $^{*}p < 0.01$ vs. SCI; $^{**}p < 0.01$ vs. SCI; and $^{***}p < 0.001$ vs. SCI.